Supporting Information

Biswas et al. 10.1073/pnas.1111498108

SI Materials and Methods

Two-Step FLAG-HA Protein Complex Purification, Mass Spectrometry Analysis, and Coimmunoprecipation Analyses. Stable cell lines that express the epitope-tagged proteins either constitutively or inducibly were made using the Flp-293 system (Invitrogen). Inducible cell lines were employed for epitope-tagged AF4 and ELL because constitutive expression of these proteins is toxic to cells. Nuclear extracts from these stable cell lines were subjected to a first round immuno-affinity purification on M2-agarose beads in binding buffer (50 mM Tris, pH 8.0, 300 mM KCl, 2 mM EDTA, 0.1% NP40, and 20% glycerol). Bound proteins were washed three times with binding buffer and eluted with FLAG peptide at 150 ng/μL. Eluted proteins were diluted 1:10 in binding buffer and subjected to a second round of immuno-affinity purification on HA-agarose beads (Sigma). After binding, the beads were washed three times with binding buffer and eluted with HA peptide at 1 μg/μL. Eluted proteins were analyzed on 4–12% SDS/PAGE gels (Bistris, Invitrogen) with silver staining and subsequently identified by tandem mass spectrometry as described earlier (1). The purified proteins were subjected to immunoblotting employing antibodies as indicated.

In Vitro Transcription Elongation, C-terminal Domain (CTD) Kinase and Histone Methyl Transferase Assays. In vitro transcription elongation assays using the purified/reconstituted proteins/complexes were performed using the protocol described by Cheng and Price (2). For the kinetic analyses, chase reactions were stopped using the stop buffers at the specified time points. For the kinase assay, purified protein complexes from 293 cells or purified reconstituted complexes from Sf9 cells were incubated at 30 °C for 1 h in kinase buffer (50 mM Tris, pH 7.5, 7 mM $MgCl_2$, 5 mM DTT, and 100 μM ATP) in the presence of 100 ng GST-CTD substrate. Reaction products were analyzed by immunoblotting with antibody specific to the phosphorylated serine 2 of the CTD repeat. Histone methyl transferase assays using an H2B-ubiquitylated nucleosome substrate were performed as described by McGinty et al. (3).

Baculovirus Expression-Based Reconstitution of Protein Complexes and Protein-Protein Interaction Analyses. Baculoviruses expressing individual factors were used for infection of Sf9 cells either alone or in the indicated combinations. Cells were harvested 48 h after infection and protein complexes were purified, through FLAG-tagged subunits, as described by Kim et al. (4). Purified complexes were analyzed on 4–12% SDS/PAGE gels (Bistris, Invitrogen) with Coomassie blue staining and/or immunoblotting.

HOXA9 Expression and Comprehensive Chromatin Immunoprecipitation (ChIP) Analyses. Whole cell extracts from primary murine bone marrow cells transduced with retroviruses expressing FLAG-HA mixed lineage leukemia 1 protein (MLL)–AF9 fusion proteins were analyzed directly for HOXA9 protein expression by immunoblot with HOXA9 antibody (Millipore) along with actin as a control. ChIP analyses were carried out as described by Milne et al. (1), but with one modification: MLL (N terminus), AF4, AFF4, and AF9 ChIP experiments were done using a double fixation method using a 2 mM ethylene glycol bis[succinimidylsuccinate] for 45 min fixation followed by a 1 h 1% formaldehyde fixation.

Hematopoietic Cell Transformation Assays. Protocols for the culture of primary murine hematopoietic stem/progenitor cells were previously described (5). In brief, 100,000 lineage-negative bone marrow stem/progenitor cells were subjected to retroviral infection, followed by kinetic analyses of proliferation versus differentiation.

1. Milne TA, et al. (2010) Multiple interactions recruit MLL1 and MLL1 fusion proteins to the HOXA9 locus in leukemogenesis. *Mol Cell* 38:853–863.
2. Cheng B, Price DH (2007) Properties of RNA polymerase II elongation complexes before and after the P-TEFb-mediated transition into productive elongation. *J Biol Chem* 282:21901–21912.
3. McGinty RK, Kim J, Chatterjee C, Roeder RG, Muir TW (2008) Chemically ubiquitylated histone H2B stimulates hDot1L-mediated intranucleosomal methylation. *Nature* 453:812–816.
4. Kim J, Guermah M, Roeder RG (2010) The human PAF1 complex acts in chromatin transcription elongation both independently and cooperatively with SII/TFIIS. *Cell* 140:491–503.
5. Wang GG, et al. (2009) Haematopoietic malignancies caused by dysregulation of a chromatin-binding PHD finger. *Nature* 459:847–851.

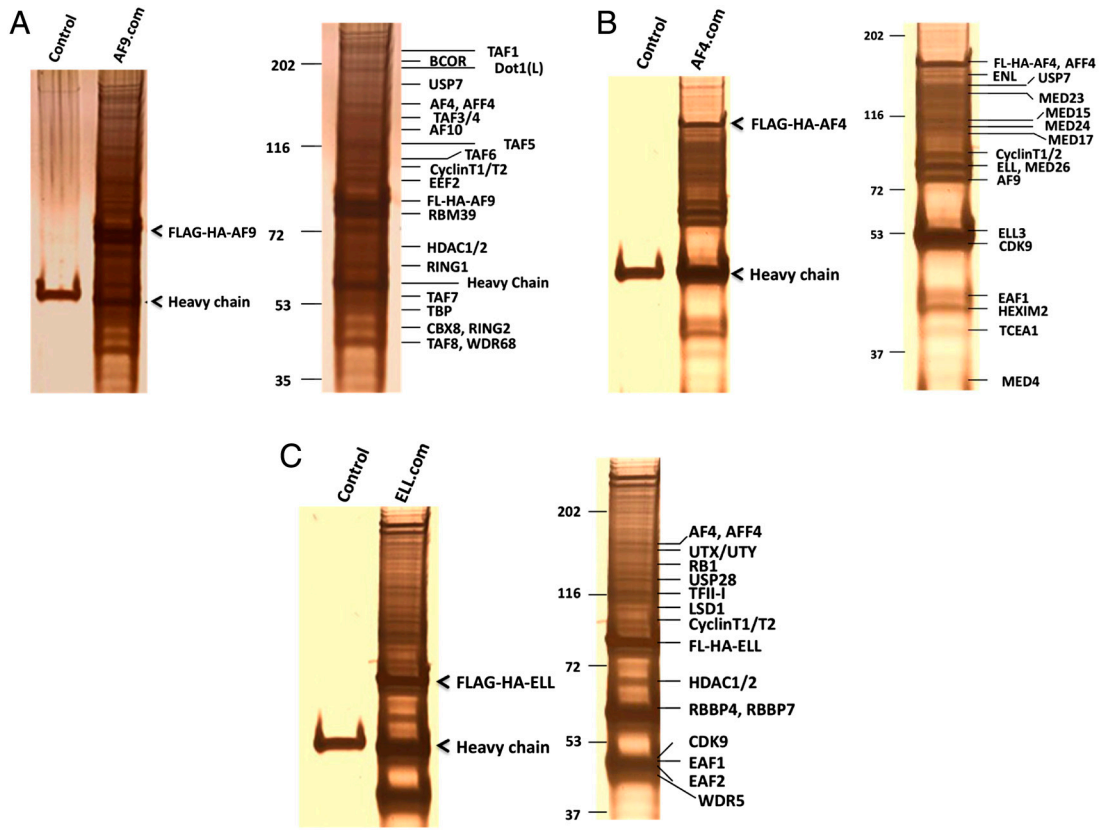

Fig. S1. Affinity purification and mass spectrometry analyses of the AF9, AF4, and ELL complexes from 293 cells (*A*, *B*, and *C*). Two-step purification of AF9 (*A*), AF4 (*B*), and ELL (*C*) complexes from a 293 cell line that stably expresses FLAG-HA-tagged AF9, AF4, and ELL proteins. The purified complexes were analyzed on 4–12% SDS/PAGE gels with silver staining. The two-step purified AF4 and ELL samples along with a mock control sample (nuclear extract from control 293 cells) were run on the same analytical gel and visualized by silver staining. For easier presentation, the ELL lane was split from the adjacent control and AF4 lanes (presented unseparated in *B*) and shown with the reproduced control lane in *C*. Polypeptides in the bands were identified by tandem mass spectrometry.

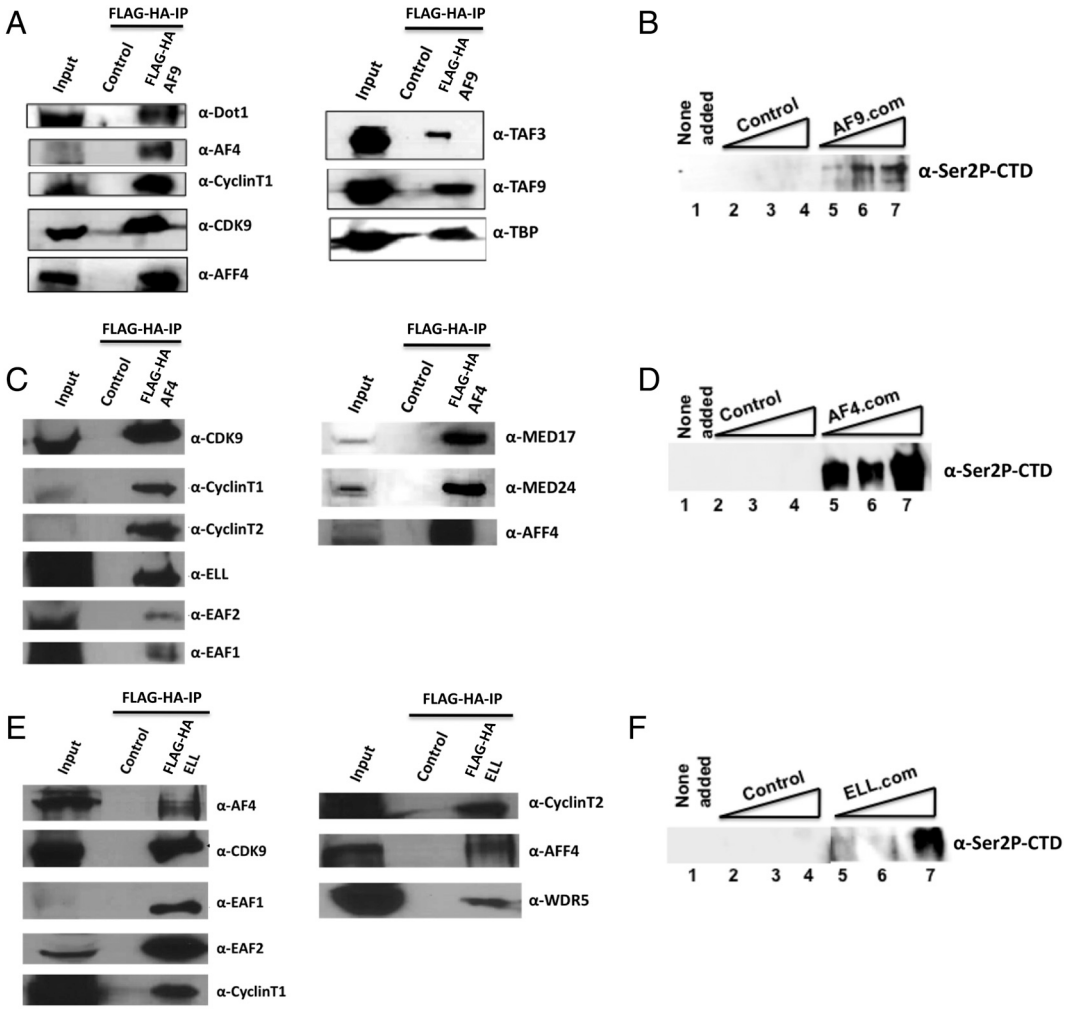

Fig. S2. Compositional (immunoblot) and functional (CTD kinase) analyses of the affinity-purified AF9, AF4, and ELL complexes from 293 cells (*A*). Immunoblot confirmation of factors in the FLAG-HA-AF9 purified complex (Fig. 1*A*) using the indicated antibodies. (*B*) In vitro CTD kinase assay using the purified AF9 complex (Fig. 1*A*). (*C*) Immunoblot confirmation of factors in the FLAG-HA-AF4 purified complex (Fig. 1*C*) using the indicated antibodies. (*D*) In vitro CTD kinase assay using the purified AF4 complex (Fig. 1*C*). (*E*) Immunoblot confirmation of factors in the FLAG-HA-ELL purified complex (Fig. 1*E*) using the indicated antibodies. (*F*) In vitro CTD kinase assay using the purified ELL complex (Fig. 1*E*).

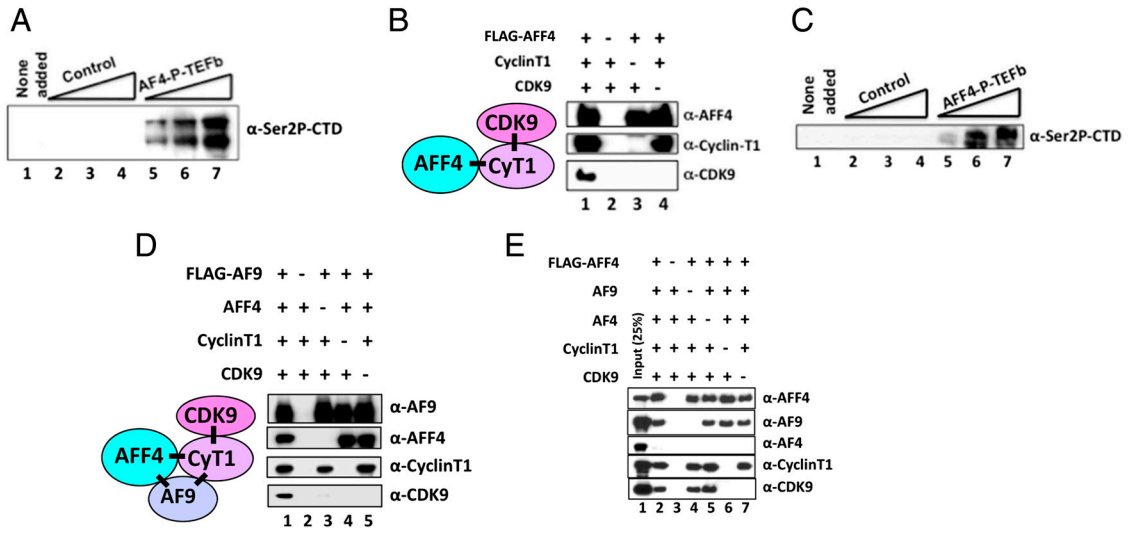

Fig. S3. Reconstitution of defined higher order complexes containing AFF4 in association with positive transcription elongation factor b (P-TEFb) and AF9 and CTD kinase assays of reconstituted AF4•P-TEFb and AFF4•P-TEFb complexes. (*A*) In vitro CTD kinase assay with the purified reconstituted AF4•P-TEFb complex (Fig. 2*A*). (*B*) Immunoblot analysis of the reconstituted AFF4•P-TEFb complex and corresponding subunit interactions. Sf9 cells were coinfected, as indicated, with baculoviruses that express FLAG-AFF4, His-cyclinT1, and His-Cdk9 and complexes were purified on M2 agarose. (*C*) In vitro CTD kinase assay using the purified reconstituted AFF4•P-TEFb complex. (*D*) Immunoblot analysis of the reconstituted AF9•AFF4•P-TEFb complex and corresponding subunit interactions. Sf9 cells were coinfected, as indicated, with baculoviruses that express FLAG-AF9, His-AFF4, His-cyclinT1, and His-Cdk9 and complexes were purified on M2 agarose. (*E*) Immunoblot analysis indicating that AF4 and AFF4 do not reside in a common complex with AF9 and P-TEFb. Sf9 cells were coinfected as indicated, with baculoviruses that express FLAG-AFF4, untagged AF9, untagged AF4, His-cyclinT1, and His-Cdk9 and complexes were purified on M2 agarose.

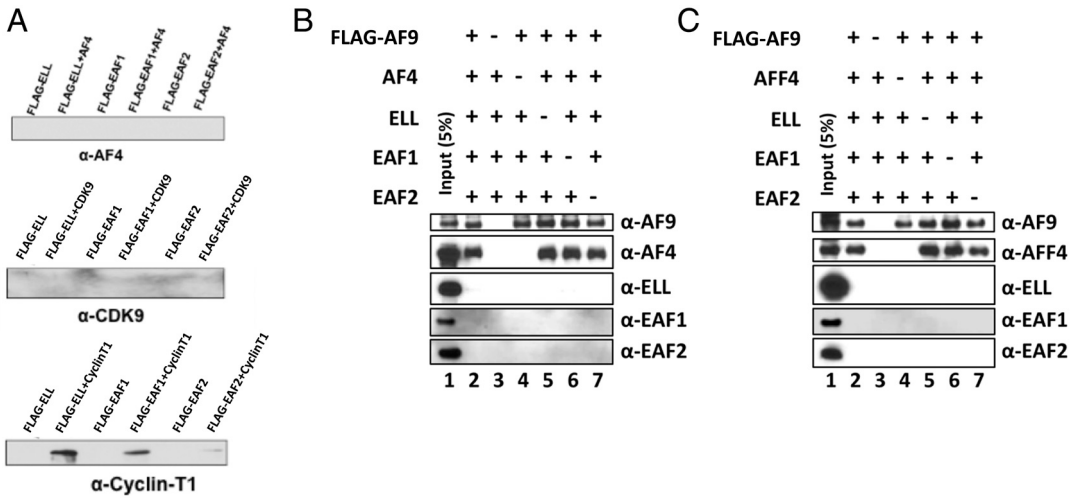

Fig. S4. Selective and direct interactions of ELL and ELL-associated factors 1 and 2 (EAF1 and EAF2) subunits with the cyclinT1 component of the AF4 and positive transcription elongation factor b (P-TEFb) complex and failure of the ELL•EAF1/2 complex to associate with AF9 in the presence or absence of AF4 or AFF4. (*A*) Immunoblot analysis of direct interactions between components of the ELL•EAF1/2 complex and components of the AF4•P-TEFb complex. Sf9 cells were coinfected with baculoviruses expressing the indicated proteins and interacting factors were purified on M2 agarose and probed with antibodies indicated at the bottom of each panel. (*B* and *C*) Immunoblot analyses indicating that AF9 and the ELL•EAF1/2 complex do not interact directly or assemble in a common complex either in presence or absence of AF4 (*B*) or AFF4 (*C*). Sf9 cells were coinfected, as indicated, with baculoviruses that express FLAG-AF9, untagged AF4 or AFF4, untagged ELL, untagged EAF1, and untagged EAF2 and complexes were purified on M2 agarose and probed with the indicated antibodies.

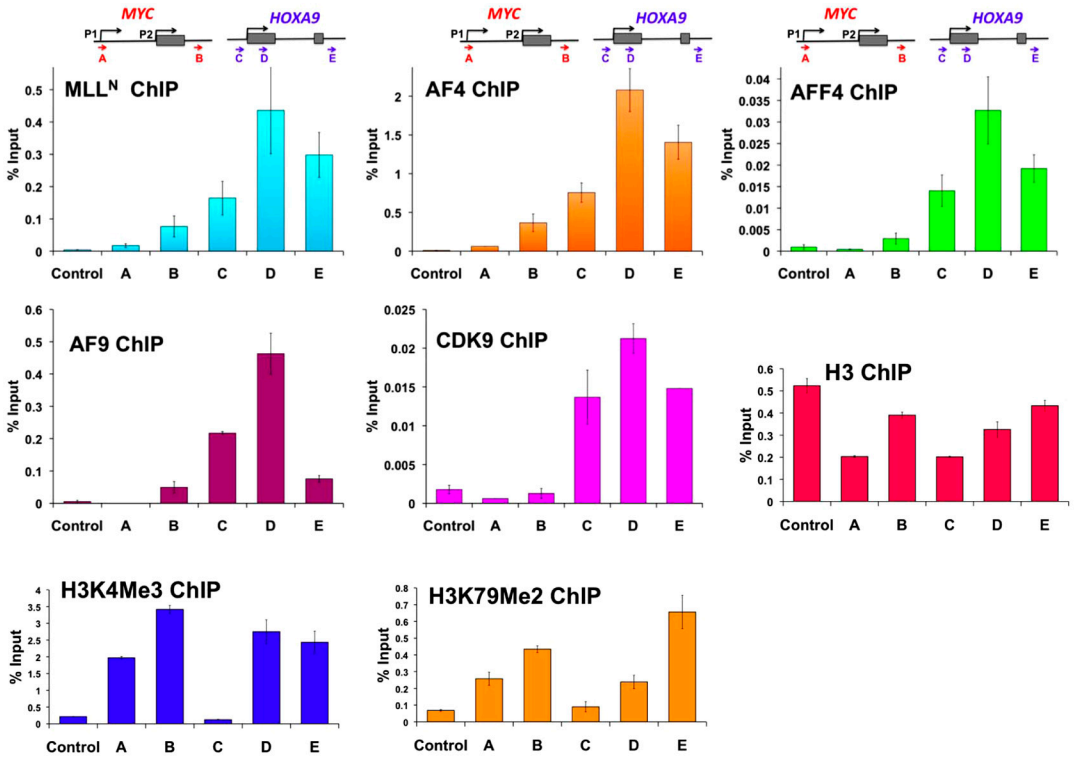

Fig. S5. ChIP analyses of fusion partners at target loci in MLL–AF4 leukemic cells. ChIP analysis of factor interactions and histone modifications at different regions of the *c-MYC* and *HOXA9* loci in RS4;11 cells containing MLL–AF4 fusion. The specific factors and histone modifications analyzed are indicated within each panel and the primers employed are indicated in the upper diagram. The signal was calculated as percent of input chromatin and bar graph values represent the average of three independent, replicate ChIP experiments. Error bars represent the standard deviation of values between experiments.

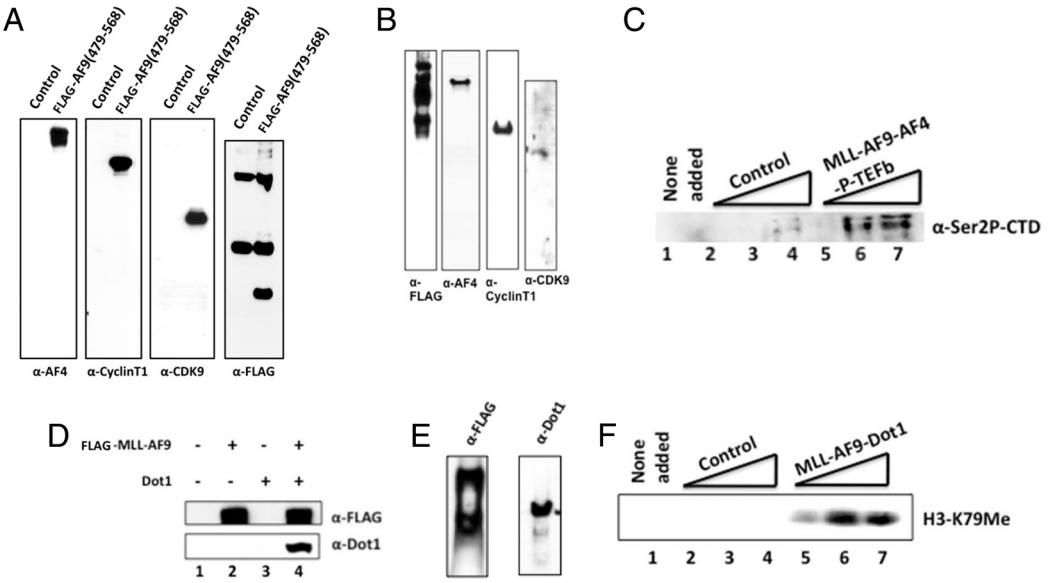

Fig. S6. Compositional (immunoblot) and functional (CTD kinase) analyses of purified reconstituted higher order complexes containing either the minimal AF9 fragment or the corresponding MLL–AF9 fusion protein. (*A*) Immunoblot analyses of the reconstituted AF9(479–568)•AF4•positive transcription elongation factor b (P-TEFb) complex described in Fig. 4*B*. (*B*) Immunoblot analyses of the reconstituted MLL–AF9(479–568)•AF4•P-TEFb complex described in Fig. 4*D*. (*C*) Immunoblot analysis of the CTD kinase activity of the purified reconstituted MLL–AF9–AF4•P-TEFb complex described in Fig. 4*D*. (*D*) Immunoblot analysis of the reconstituted MLL–AF9•DOT1 complex. Sf9 cells were coinfected with baculoviruses that express FLAG-MLL–AF9 and His–DOT1 and interacting proteins were purified on M2 agarose. (*E*) Immunoblot analyses of the reconstituted MLL–AF9•DOT1 complex described in Fig. 4*F*. (*F*) Histone methyl transferase activity of the purified reconstituted MLL–AF9•DOT1 complex using radioactive *S*-adenosylmethionine (AdoMet).

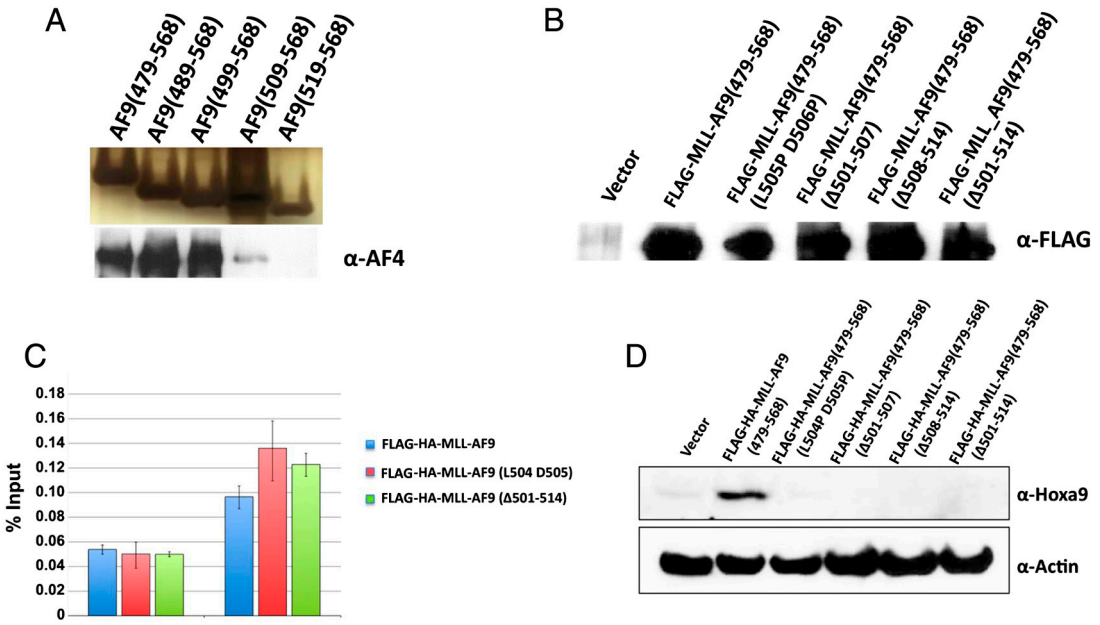

Fig. S7. Mutational analyses of minimal AF9 fragment for its association with AF4 by baculovirus coinfections, expression and recruitment analyses of some of the MLL–AF9 mutants in 293 cells, and HOXA9 expression analysis in the transduced murine progenitor bone marrow cells. (*A*) Expression in Sf9 cells of AF9 C-terminal fragments (SDS/PAGE with silver staining, *Top*) and interactions with coexpressed AF4 (immunoblot with anti-AF4 antibody, *Bottom*). Sf9 cells were coinfected, as indicated, with baculoviruses that express untagged AF4 and the indicated FLAG-AF9 fragments and complexes were purified on M2 agarose. (*B*) Expression in 293 cells (immunoblot with anti-FLAG antibody) of the FLAG-HA-MLL•AF9 constructs that were used for the hematopoietic transformation assays in Fig. 5*D*. (*C*) ChIP analysis showing recruitment of ectopic wild-type and mutant MLL–AF9 proteins to the target *HOXA9* locus in 293 cells. Antibody specific to the HA epitope-tag of the MLL–AF9 fusion constructs (Fig. 5*D*) was employed. (*D*) Analysis of HOXA9 expression in murine primary bone marrow cells after transduction with retroviruses carrying MLL–AF9 or the indicated MLL–AF9 mutants.